NONLINEAR DYNAMIC ANALYSIS OF A SLENDER FRAME UNDER REAL AND SYNTHETIC SEISMIC EXCITATIONS CONSIDERING THE BASE WITH ELASTO-PLASTIC BEHAVIOR

Luis F. Paullo Munoz

Paulo B. Gonçalves

lf_pm21@hotmail.com

paulo@puc-rio.br

Civil Engineering Department, Pontifical Catholic University of Rio de Janeiro

Rua Marquês de São Vicente 225, 22451-900, Rio de Janeiro, RJ, Brazil

Ricardo A. M. Silveira

Andréa R. D. Silva

ricardo@em.ufop.br

andreadiassilva@yahoo.com.br

Civil Engineering Department, School of Mines, Federal University of Ouro Preto

Morro do Cruzeiro, Campus Universitário s/n°, 35400-000, Ouro Preto, MG, Brazil

Abstract. *The seismic analysis has a great importance in the dynamic analysis of structures, since earthquakes are present around the world with various intensities and recurrences. A relevant topic is the consideration of a flexible base instead of a conventional fixed base. This consideration can modify palpably the structural response in terms of displacements and accelerations. One aspect that has a significant influence in dynamic response of structures under seismic loads is the relation between the power distribution of the seismic excitation and the frequency properties of the structure, since excitations with power concentration close to resonance regions of structures can produce large displacements, which may impair the structural integrity. In the present work, the dynamic response of a geometrically non-linear slender one-floor frame under real and synthetic seismic loads considering an elasto-plastic base is studied. The space problem is solved through the discretization of the structure using a beam-column finite element mesh, and the time domain response is obtained by direct integration of the resulting non-linear equations of motion.*

Keywords: *Non-linear dynamic analysis, Seismic excitation, Resonance frequencies, Time domain integration, Elasto-plastic base.*

1 INTRODUCTION

Seismic analysis is an important area structural dynamics, since earthquakes are present around the world with various intensities and recurrences. A relevant topic is the consideration of a flexible base instead of a conventional fixed base. This consideration can modify palpably the response of the structure in terms of displacements and accelerations. In this context, flexible base consideration becomes an essential topic in addressing problems of structures subjected to earthquakes. Several researchers have studied this phenomenon. The simplest hypothesis is to consider the base as an elastic medium represented by elastic springs as in Hetenyi (1946), Vlasov (1966) and Aristizabal-Ochoa (2003) and, recently, Nguyen (2008) and Paullo (2010). A more realistic hypothesis consists in considering the base as a continuum. Alsaleh Shahrour (2009) and Clouteau et al. (2012) studied these problems modelling the building base as a continuous medium. A simplifying assumption is the consideration of the flexible base as discrete flexible support, which is a useful hypothesis when the focus lies in the study of the structure's behavior. Wolf [14], Halabian (2002), and Ganjavi and Hao (2012) studied the dynamic behavior of frames using this simplified assumption.

The study of the geometric nonlinearity of structures has been an important issue in structural analysis, in particular, in the case slender arches and frames. In the study of geometric nonlinearity, the formulations are classified according to the type of reference used. Distinct researchers have developed formulations in total or updated Lagrangian reference. Galvão (2000, 2004) and Silva (2009) highlight the works published by Loi and Wong (1990), and Pacoste and Erikson (1995) as significant contributions in the development Lagrangian formulations for frame structures. Comparisons between different geometric nonlinear formulations have also attracted the interest of many researchers (Galvão, 2000). In this article, only the updated Lagrangian formulation is employed.

One aspect that has a great influence in dynamic response of structures under seismic loads is the relation between the power distribution of the seismic excitation and the frequency properties of the structure. Since excitations with power concentrated in regions close to the structure's resonance regions can produce large displacements, and, as a consequence, may impair the structural integrity. In this context, the study of the phase variation in the seismic acceleration is a relevant topic, since this variation can modify the response in term of the structure's displacement and the acceleration. For this, the generation of synthetic earthquakes is a useful tool. Clough and Penzien (1995), and Roehl (2000) present a numerical procedure for the generation of synthetic acceleration registers based on the superposition of harmonic functions with random phase parameters.

The aim of the present contribution is to study the dynamic response of a slender one-floor geometrically non-linear frame under real and synthetic seismic loads considering an elasto-plastic base. The space problem is solved through the discretization of the structure using a beam-column finite element mesh, and the time domain response is obtained by direct integration of the resulting non-linear equations of motion.

2 FORMULATION

2.1 Equations of motion

In the finite element context, the non-linear equations of motion of the structural model is given by:

$$\boldsymbol{M}\ddot{\boldsymbol{u}}(t) + \boldsymbol{C}.\dot{\boldsymbol{u}}(t) + \boldsymbol{Fi}(t) = \boldsymbol{Fe}(t) \tag{1}$$

where $\boldsymbol{u}$, $\dot{\boldsymbol{u}}$ and $\ddot{\boldsymbol{u}}$ are the nodal displacement, velocity and acceleration vectors, respectively; $\boldsymbol{M}$ and $\boldsymbol{C}$ are the mass and the damping matrices, respectively; $\boldsymbol{Fi}$ is the vector of internal forces, and $\boldsymbol{Fe}$ is the vector of nodal external equivalent forces. The matrices $\boldsymbol{M}$ and $\boldsymbol{C}$ are obtained as:

$$\boldsymbol{M} = \int_V \rho \boldsymbol{H}(x)^{\mathrm{T}} \boldsymbol{H}(x) dV \, , \boldsymbol{C} = \int_V c \boldsymbol{H}(x)^{\mathrm{T}} \boldsymbol{H}(x) dV \tag{2}$$

where ρ and c are the mass density and damping coefficient, respectively, and $\boldsymbol{H}(x)^{\mathrm{T}}$ is the matrix that contain the shape functions which define the displacement field approximation. In the present work, Hermitian shape functions are used for the flexural displacements and linear functions for the axial displacements. More details can be found in Silva (2009) and Galvão (2004).

In seismic analyses, the external force is composed by inertial forces due to the base displacement field (Clough and Penzien, 1996). Thus, it is convenient to define as the problem unknown the displacement field responsible for the deformations in the structure. In this context, Eq. (1) can be rewritten as:

$$\boldsymbol{M}\ddot{\bar{\boldsymbol{u}}}(t) + \boldsymbol{C}.\dot{\bar{\boldsymbol{u}}}(t) + \boldsymbol{Fi}(t) == -\boldsymbol{M}\mathbf{r}\ddot{u}_g(t) \tag{3}$$

were $\bar{\boldsymbol{u}}$ is the nodal displacement vector related to the base displacement, $\ddot{u}_g$ is the seismic acceleration and $\mathbf{r}$ is the vector that define the degrees of freedom which are excited by the base displacement (Villa Verde, 2008).

2.2 Elasto-plastic base model

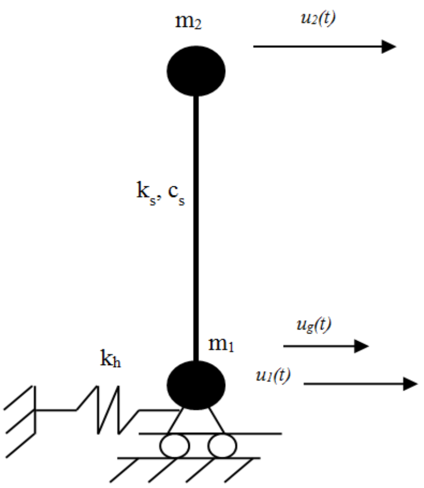

Figure 1. Discrete model of system with flexible base.

Consider initially that the structure base flexibility can be represented by a discrete horizontal spring with stiffness k_h, as shown in Figure 1. In the case of a conventional fixed base, that is, when k_h tends to infinity, the displacement u1(t) = 0 and the system can be reduced to a one degree of freedom model described by the following equation:

$$m_2.\ddot{u}_2(t) + c_s\dot{u}_2(t) + k_s u_2(t) = -m_2\ddot{u}_g(t) \tag{4}$$

by imposing the condition u1(t) = 0. However, when u1(t) is nonzero, the entire system must be considered. In such case:

$$\begin{bmatrix} m_1 & 0 \\ 0 & m_2 \end{bmatrix} . \begin{Bmatrix} \ddot{u}_2 \\ \ddot{u}_1 \end{Bmatrix} + \begin{bmatrix} c_s & -c_s \\ -c_s & c_s \end{bmatrix} \begin{Bmatrix} \dot{u}_2 \\ \dot{u}_1 \end{Bmatrix} + \begin{bmatrix} k_s & -k_s \\ -k_s & k_s \end{bmatrix} \begin{Bmatrix} u_2 \\ u_1 \end{Bmatrix} = -\begin{Bmatrix} m_1 \\ m_2 \end{Bmatrix} \ddot{u}_g \tag{5}$$

Adding the base stiffness and damping to the corresponding degrees of freedom, results in:

$$\begin{bmatrix} m_1 & 0 \\ 0 & m_2 \end{bmatrix} . \begin{Bmatrix} \ddot{u}_2 \\ \ddot{u}_1 \end{Bmatrix} + \begin{bmatrix} c_s & -c_s \\ -c_s & c_s + c_h \end{bmatrix} \begin{Bmatrix} \dot{u}_2 \\ \dot{u}_1 \end{Bmatrix} + \begin{bmatrix} k_s & -k_s \\ -k_s & k_s + k_h \end{bmatrix} \begin{Bmatrix} u_2 \\ u_1 \end{Bmatrix} = -\begin{Bmatrix} m_1 \\ m_2 \end{Bmatrix} \ddot{u}_g \tag{6}$$

Generalizing for a system with *n* degrees of freedom, the inclusion of the deformable base can be obtained by adding a diagonal stiffness and damping matrix term corresponding to the degrees of freedom of the base. Then, the system described in Eq. (3) can be modified to:

$$\boldsymbol{M}\ddot{\bar{\boldsymbol{u}}}(t) + (\boldsymbol{C} + \boldsymbol{C_s})\,\dot{\bar{\boldsymbol{u}}}(t) + (\boldsymbol{K} + \boldsymbol{K_s})\bar{\boldsymbol{u}}(t) = -\mathbf{Mr}\ddot{u}_g(t) \tag{7}$$

2.3 Internal force vector

In the FE context, the nodal internal forces vector is obtained by integration of the stresses due to the elastic deformation of structure, that is:

$$\boldsymbol{F_i} = \int_V \boldsymbol{B}^{\mathrm{T}} \boldsymbol{\tau} dx \tag{8}$$

were $\boldsymbol{\tau}$ are the structure's stress field and $\boldsymbol{B}$ is the kinematic strain-displacement matrix. Its determination depends on the non-linear kinematic formulation (see Silva (2009) and Galvão (2004) for more details). Integrating the equations of motion step by step, the vector of internal forces, $\boldsymbol{F_i}$, at a time t+Δt, is given by:

$${}^{t+\Delta t}\boldsymbol{F_{int}} = {}^{t}\boldsymbol{F_{int}} + \Delta\boldsymbol{F_{int}},\ \Delta\boldsymbol{F_{int}} = \mathbf{K}(\bar{\boldsymbol{u}}).\Delta\bar{\boldsymbol{u}} \tag{9}$$

where $\Delta\bar{\boldsymbol{u}}$ is the incremental nodal displacement vector, $\mathbf{K}(\bar{\boldsymbol{u}})$ is the stiffness matrix, which depends on the nodal displacement and contains the linear and nonlinear geometric effects. In this paper, a linearized formulation for geometric nonlinear effects is adopted, and $\mathbf{K}$ depends on the internal forces (Silva, 2009).

2.4 Synthetic seismic acceleration

Synthetic seismic excitations can be generated from the power spectral density function (PSDF) of a real earthquake (Villaverde, 2008). For this, a harmonic function superposition scheme is adopted. The PSDF of the earthquake acceleration is defined as:

$$\phi_{ff}(\omega) = \frac{1}{2\pi T}\left|\int_0^T \ddot{u}_g(t)\, e^{-i\omega t} dt\right|^2 \tag{10}$$

where T is the period, which in this case corresponds to the earthquake duration.

For the synthetic earthquake generation, the following harmonic function $x_i(t)$ is defined:

$$x_i(t) = A_i sen(\omega_i t + \alpha_i) \tag{11}$$

where A_i is the modal amplitude, ω_i is the frequency and α_i is the phase angle. Superposing the harmonic functions, the synthetic seismic acceleration is obtained as:

$$\ddot{u}(t) = \sum_{i=1}^{N} x_i(t) \tag{12}$$

Equation (12) defines the synthetic acceleration shape, which corresponds to a sinusoidal Fourier series, and the amplitude A_i is given by:

$$A_i = \phi_{ff}(\omega_i) \tag{13}$$

The random characteristic of the process is given by the phase angle determination, and is obtained through a pseudo-random number generator, which use the following recurrence formula:

$$x_i := m\left(\frac{a\,x_{i-1}+c}{m} - \text{floor}\left(\frac{a\,x_{i-1}+c}{m}\right)\right) \tag{14}$$

where x_i is a real number with value between 0.0 and 1, x_0 is the initial value of the generator, m is the total of numbers which are generated, the operator floor(..) gives de absolute value of the most close integer number, and a and c are the coefficients which depend on the kind of distribution. It is adopted here a uniform distribution for the phase angle generation with $a = c = 255$ (Fisher, 2011). Finally, the phase angle can be obtained as:

$$\alpha_i = x_i.2\pi \tag{15}$$

Finally, a correction process due to initial and final conditions, as well as its normalization with respect to a desired maximum acceleration is employed. Paullo (2015) gives more details on this synthetic acceleration generation process.

2.5 Direct integration of the equation of motion

In the present work, the structural time response is obtained by the direct integration of the equations of motion by the implicit fourth-order Runge-Kutta method together with a two-steps procedure using the coefficients presented in Butcher (2003), obtained by means of the Gaussian quadrature. The method is adapted here to the nonlinear system, which is solved in conjunction with an iterative secant-type procedure (Paullo, 2015).

3 NUMERICAL EXAMPLES

In this section, the dynamic response of a plane one-floor frame under the action of two groups of seismic loads is studied. The structure is modeled by 20 Euler-Bernoulli beam-column elements, being 6 equal elements used for the roof and 7 equal elements for each column. In addition, the elasto-plastic behavior of the rotational degrees of freedom at the structure base is considered. The geometry and material parameters, as well as the elasto-plastic parameters are shown in Figure 2.

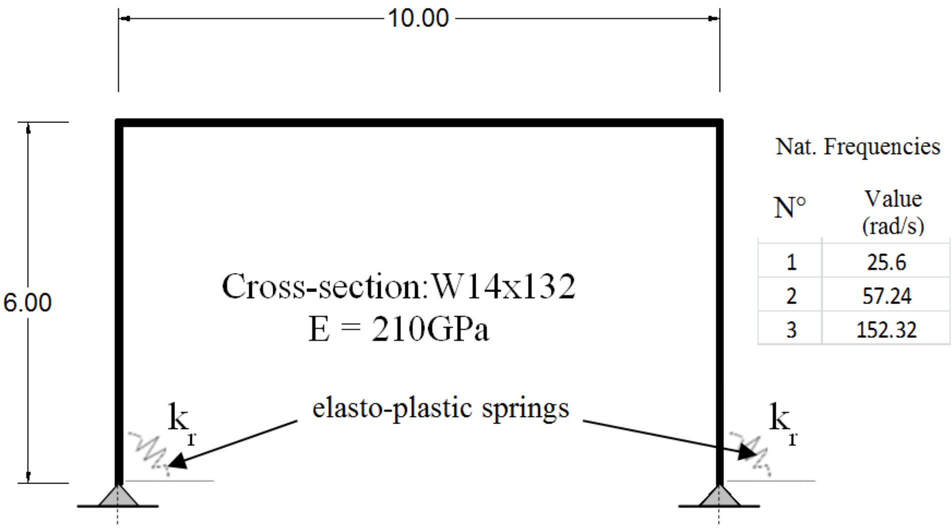

Figure 2. Geometry of the plane frame and elasto-plastic parameters: $k_r = 5 * 10^{10} Nm/rad$, $k^{ep} = 0.1 * k_r$, $Mp = 10^5 Nm$ (dimensions in meters)

3.1 Real seismic excitation

Two earthquakes are taken as dynamic excitation. The first one is the component north-south of the earthquake El Centro (California, 1940) and the component east-west of the earthquake Kobe (1995). The earthquake El Centro is often used as a representative seismic load example (Villaverde, 2009); the earthquake Kobe is a relatively more recent event, and has taken the scientific community attention because of its big negative effects over the structural systems (high acceleration with the collapse of important buildings; Villaverde, 2009). Figure 3 shows the seismic acceleration and the correspondent power spectral density function of these earthquakes.

3.2 Synthetic seismic loads

Five earthquakes acceleration are generated for the two considered real earthquakes. The synthetic seismic accelerations are generated varying the initial value x_0 in the random number generation process to phase angle determination. They are: x_0 = 5, 10, 20, 50 and 100. It is important to point out that the synthetic accelerations have the same power spectral density of the original real earthquakes. The synthetic accelerations are identified using the following names: SAEC1, SAEC2, SAEC3, SAEC4 and SAEC5 for the acceleration obtained from the earthquake El Centro, and SAKB1, SAKB2, SAKB3, SAKB4 and SAKB5 for the acceleration obtained from earthquake Kobe. All the synthetic seismic events have 30 min of duration. In all examples, it is considered that the vertical component of earthquake acceleration is 0.66 times of the horizontal component, following the criteria of the same earthquake codes, such as Peruvian Seismic Analysis and Design Code (RNE-E030, 2006). The synthetic seismic acceleration SAEC1 and SAKB1 are shown in Figure 4.

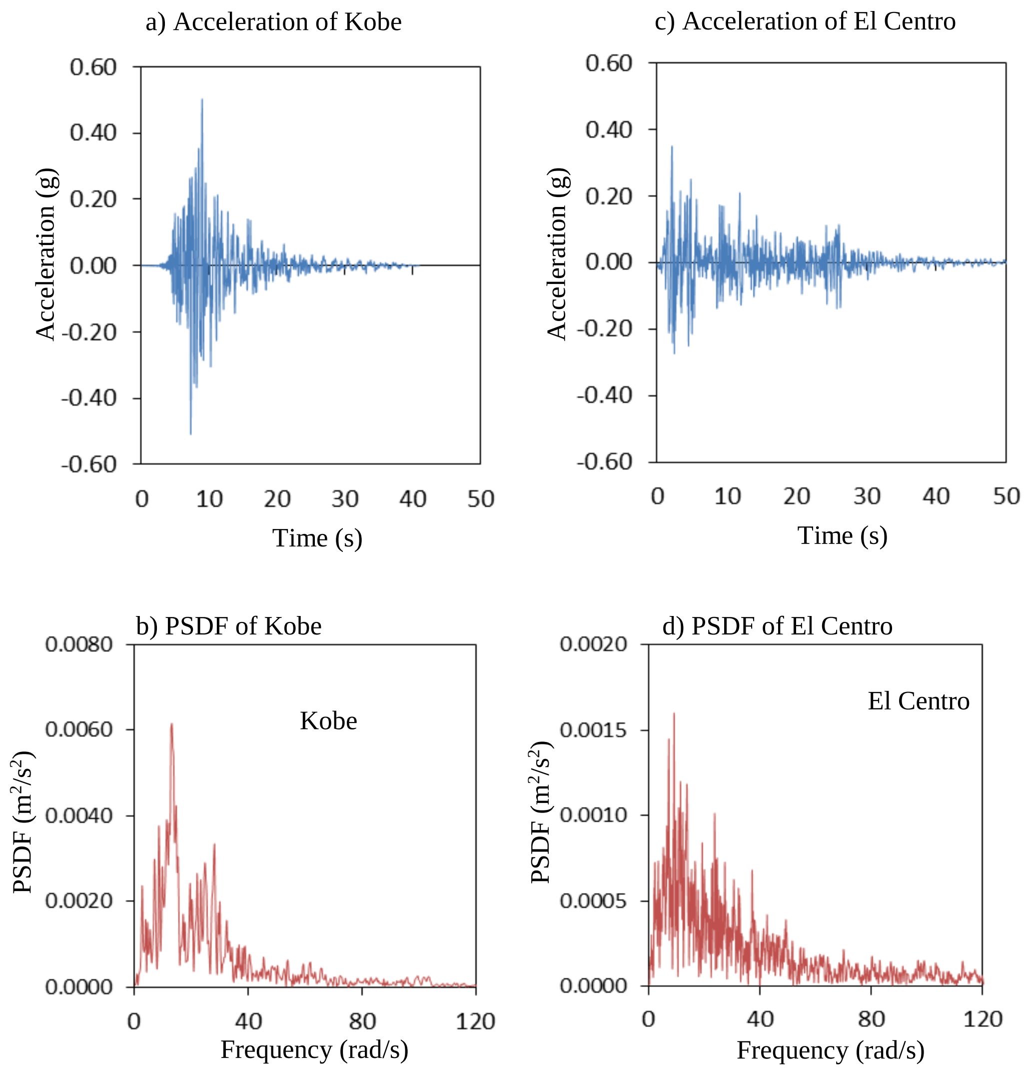

Figure 3. a) East-west component acceleration of earthquake Kobe; b) PSDF of earthquake Kobe; c) North-south component acceleration of earthquake El Centro; and d) PSDF of earthquake El Centro.

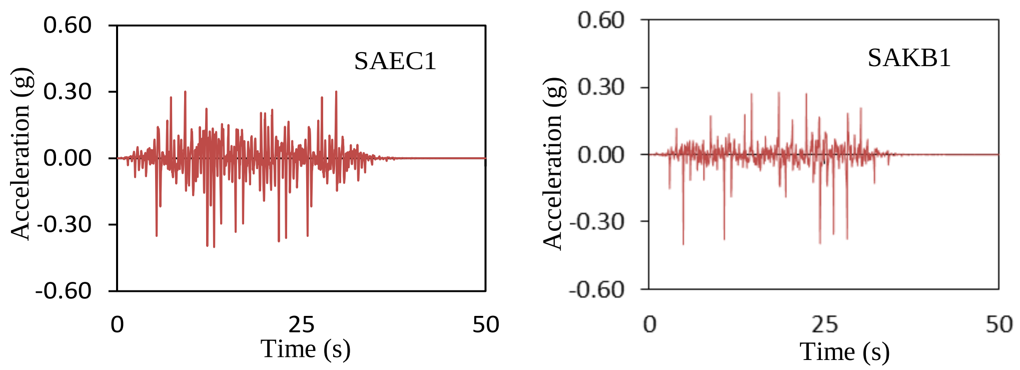

Figure 4. Synthetic seismic acceleration examples

3.3 Real excitation response

Figures 5 shows the horizontal displacement time response at the frame top obtained with the earthquakes Kobe and El Centro considering the rigid base and elasto-plastic base behavior (rotation degrees of freedom). In both of cases, the elasto-plastic base consideration produce a reduction of the displacement amplitude: 10.5% in the earthquake El Centro; and 20% in the case of the earthquake Kobe. This reduction is due to energy dissipation process in the base. Figure 5 also shows that the earthquake Kobe, which registers a maximum horizontal displacement of 0.083m, produces bigger displacements than the earthquake El Centro, which registers a maximum horizontal displacement of 0.057m. This behavior it also seen for the elasto-plastic base model.

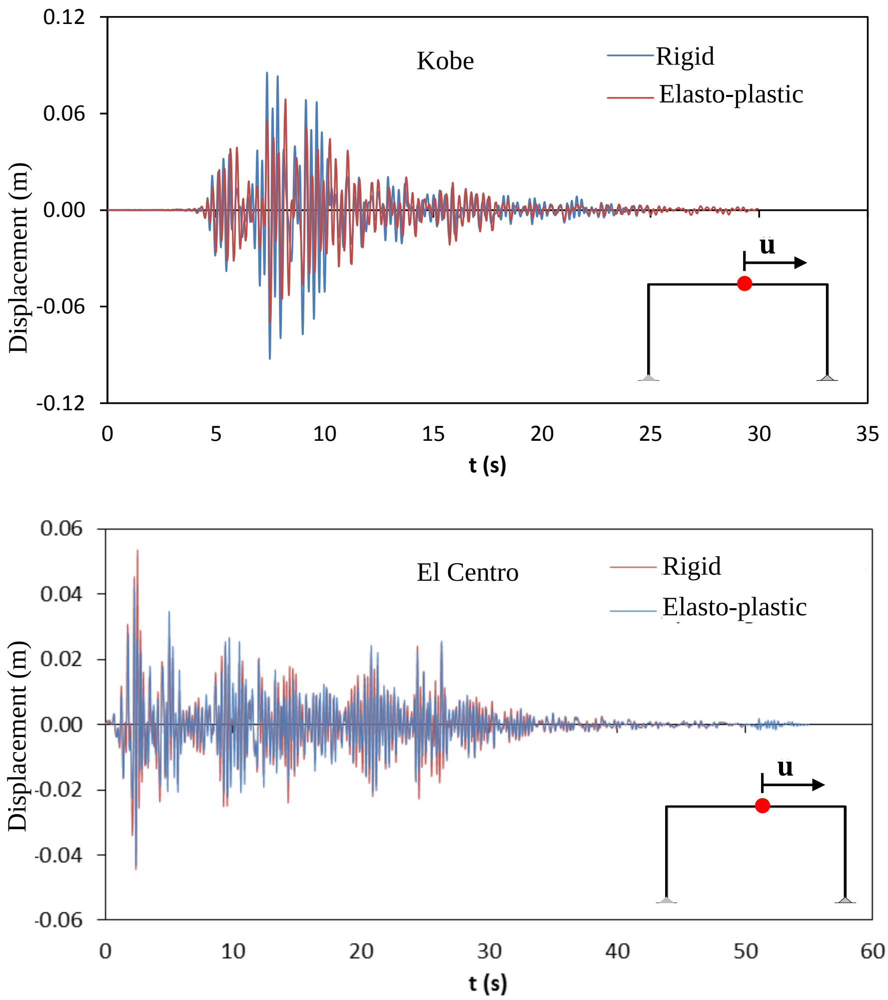

Figure 5. Horizontal displacement response at the frame top for real excitations

Figure 8 shows the horizontal displacement time response at the frame top considering the synthetic earthquakes SAKB1 and SAEC1, for the rigid and elasto-plastic base behavior. It can be observed that in both synthetic earthquakes, the rigid base cases produces the bigger horizontal displacement, showing the dissipation processes. Also note that the earthquake SAKB1 produce a bigger maximum displacement than the SAEC1. Both synthetic earthquakes exhibit bigger displacement than the correspondent real seismic excitations.

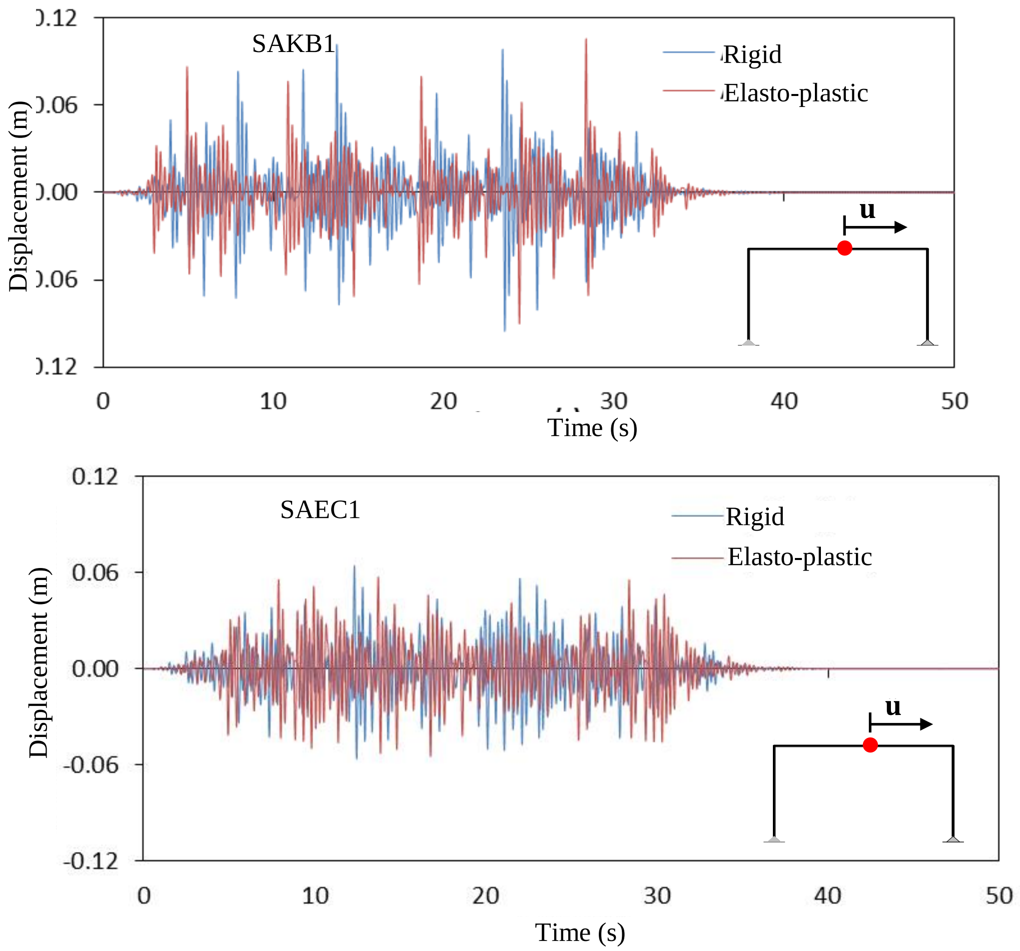

Figure 6. Horizontal displacement response at the frame top for synthetic excitations

Tables 1 and 2 present the maximum horizontal displacement and horizontal acceleration at the structure top obtained with the real and synthetic earthquakes, as well as the amplification factor in terms of the maximum acceleration. It can be seen an important variability on these values, noting that the earthquake SAKB1 (Kobe) registers the maximum value of amplification 3.7 against the amplification factor of 2.58 in the real excitation. A similar behavior is observed in the earthquakes generates from the earthquake El Centro, where the earthquake SAEC1 produces the maximum amplification factor, 3.55, while the real excitation registers 1.50. This shows the importance of the acceleration configuration in terms of the phase angles and position of the acceleration maximum peak, which can substantially modify the structure response, even for real and synthetic earthquakes sharing the same PSDF.

Table 1. Maximum displacement and acceleration at the frame top: El Centro real and synthetic earthquakes acceleration.

Earthquake	Max. horizontal displacement (m)		Max. horizontal acceleration (g)		Amplification (g/g)	
	Rigid	Elasto-Plas.	Rigid	Elasto-Plas.	Rigid	Elasto-Plas.
El Centro	0.057	0.055	0.6	0.43	1.50	1.08
SAEC1	0.0575	0.0501	1.06	1.06	2.65	2.65
SAEC2	**0.0755**	**0.6274**	**1.40**	**1.23**	**3.50**	**3.08**
SAEC3	0.0573	0.0571	0.43	0.44	1.08	1.10
SAEC4	0.0628	0.0577	0.54	1.08	1.35	2.70
SAEC5	0.0572	0.0573	1.07	1.07	2.68	2.68

Table 2. Maximum displacement and acceleration at the frame top: Kobe real and synthetic earthquakes acceleration.

Earthquake	Max. horizontal displacement (m)		Max. horizontal acceleration (g)		Amplification (g/g)	
	Rigid	Elasto-Plas.	Rigid	Elasto-Plas.	Rigid	Elasto-Plas.
Kobe	0.083	0.078	1.29	0.93	2.580	1.860
SAKB1	**0.101**	**0.097**	**1.85**	**1.75**	**3.700**	**3.500**
SAKB2	0.075	0.0754	1.23	0.92	2.450	1.840
SAKB3	0.101	0.0921	1.72	1.90	3.448	3.800
SAKB4	0.095	0.093	1.66	1.75	3.320	3.700
SAKB5	0.092	0.0931	1.87	1.8	3.740	3.600

4 FINAL REMARKS

The consideration of the elasto-plastic behavior of the structure’s base supports lead to displacement and acceleration reduction when compared with the response considering the conventional rigid base. This behavior is due to the energy dissipation process that occurs as a function of the adopted elasto-plastic base model.

Synthetic seismic excitations generated from the same power spectral density function, based on a real earthquake signal, leads to a large variability in the structure response, in terms of the maximum displacement and maximum acceleration (as well as amplification factors). These results emphasize the influence of the random character of the seismic signal on the structural response.

ACKNOWLEDGEMENTS

The authors wish to express their gratitude to CAPES, CNPq and FAPEMIG (federal and state agencies), and PROPEC/UFOP, for the support received in the development of this research.

REFERENCES

Alsaleh, H., & Shahrour, H., 2009. Influence of plasticity on the seismic soil– micropiles–structure interaction. *Soil Dynamics and Earthquake Engineering*, vol. 29, pp. 574-578.

Aristizábal-Ochoa, J.D., 2003. Estructura de vigas sobre suelos elásticos de rigidez variable, *Revista Internacional de Desastres Naturales, Accidentes e Infraestructura Civil*, vol. 3, n. 2, pp. 157-174.

Butcher, J.C., 2008. *Numerical methods for ordinary differential equations*: *2nd ed*. John Wiley & Sons Ltd/New York.

Clough, R. W., & Penzien, J., 1995. *Dynamics of Structures*: 3rd ed, Wiley & Sons Ltd.

Clouteau, D., Brocb, D., Devésac, G., Guyonvarhc, V., & Massinc, P., 2012. Calculation methods of Structure–Soil–Structure Interaction (3SI) for embedded buildings: Application to NUPEC tests. *Soil Dynamics and Earthquake Engineering*, vol. 32, pp. 129–142.

Fisher, I., 2011. *Simulación Computacional: Generación de números aleatórios*. Course notes, Departamento de Engenharia Civil, Universidad Del Valle, Colômbia. Allowed online in 08/20/2011: http://eisc.univalle.edu.co/materias/Simulacion_Computacional/SC0.pdf.

Galvão, A. S., 2000. *Formulações Não-lineares de Elementos Finitos para Análise de Sistemas Estruturais Metálicos Reticulados Planos.* MSc. Dissertation, Civil Engineering Department /PUC-Rio. Rio de Janeiro, Brazil.

Galvão, A. S., 2004. *Instabilidade Estática e Dinâmica de Pórticos Planos com Ligações Semi-rígidas*, DSc. Thesis, Civil Engineering Department /PUC-Rio. Rio de Janeiro, Brazil.

Ganjavi, B., & Hao, H., 2012. A parametric study on the evaluation of ductility demand distribution in multi-degree-of-freedom systems considering soil–structure interaction effects. *Engineering Structures*, vol. 43, pp. 88-104.

Halabian, A.M., & Hesham El Naggar, M., 2002. Effect of non-linear soil–structure interaction on seismic response of tall slender structuresion. *Soil Dynamics and Earthquake Engineering*, vol. 22, pp. 639-658.

Hetenyi, M., 1946. *Beams on elastic Foundation*. The University of Michigan Press/Michigan.

Ministerio de Vivienda y Construção*, 2007. Reglamento Nacional De Construcciones* – RNE E030: Norma de diseño sirmorresistente. Technical code. Lima/Perú, 2007.

Nguyen, V-H., & Duhamel, D., 2008. Finite element procedure for nonlinear structures in moving coordinates. Part II: Infinite beam under moving harmonic loads. *Computers and Structures*, vol. 86, pp. 2056-2063.

Pacoste, C., & Eriksson, C., 1995. Element behavior in post-critical plane frame analysis. *Computer Methods in Applied Mechanics and Engineering*, vol. 125, pp. 319-343.

Paullo Muñoz, L.F., 2010. *Análise Dinâmica de Vigas Apoiadas em Fundação Elástica sob a Ação de Cargas Móveis*. MSc. Dissertation. Civil Engineering Department/PUC-Rio. Rio de Janeiro, Brazil.

Paullo Muñoz, L.F., 2015. *Análise Dinâmica de Não Linear de Pórticos sob Excitção Sísmica considerando Base Elasto-plástica*. DSc. Thesis. Civil Engineering Department/PUC-Rio. Rio de Janeiro, Brazil.

Silva, A.R.D., 2009. *Sistema Computacional para Análise Avançada Estática e Dinâmica de Estruturas Metálicas*. DSc. Thesis. Departamento de Engenharia Civil/ Escola de Minas/UFOP, Ouro Preto, Brazil.

Silveira, R.A.M., 1995. *Análise de Elementos Estruturais Esbeltos com Restrições Unilaterais de Contato.* Dsc Thesis, Civil Engineering Department/PUC-Rio. Rio de Janeiro. Brazil.

Villaverde, R., 2009. *Fundamental Concepts of Earthquake Engineering*. Taylor and Francis Group/USA.

Vlasov, V.Z., & Leontiev, N.N., 1966. *Beams, plates and Shells on elastic foundations*. Program for Scientific Translation/Jerusalem,Israel.

Wolf, J.P., 1994. *Foundation Vibration Analysis Using Simple Physical Models*. Prentice-Hall/New Jersey.

Wong, M.B. & Tin-Loi, F. E., 1990. Analysis of frames involving geometrical and material nonlinearities. *Computers & Structures,* vol. 34, n. 4, pp. 641-646.